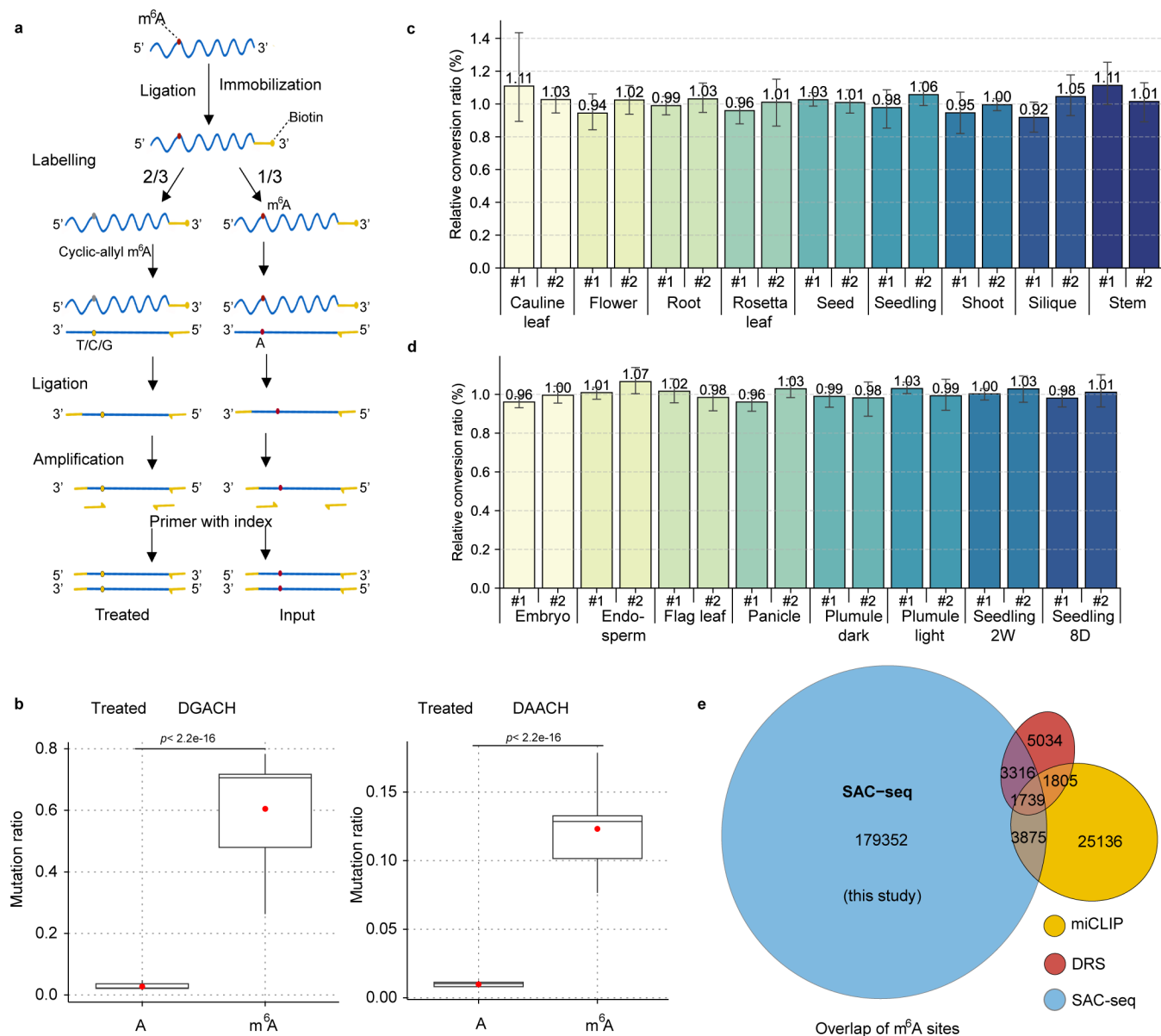
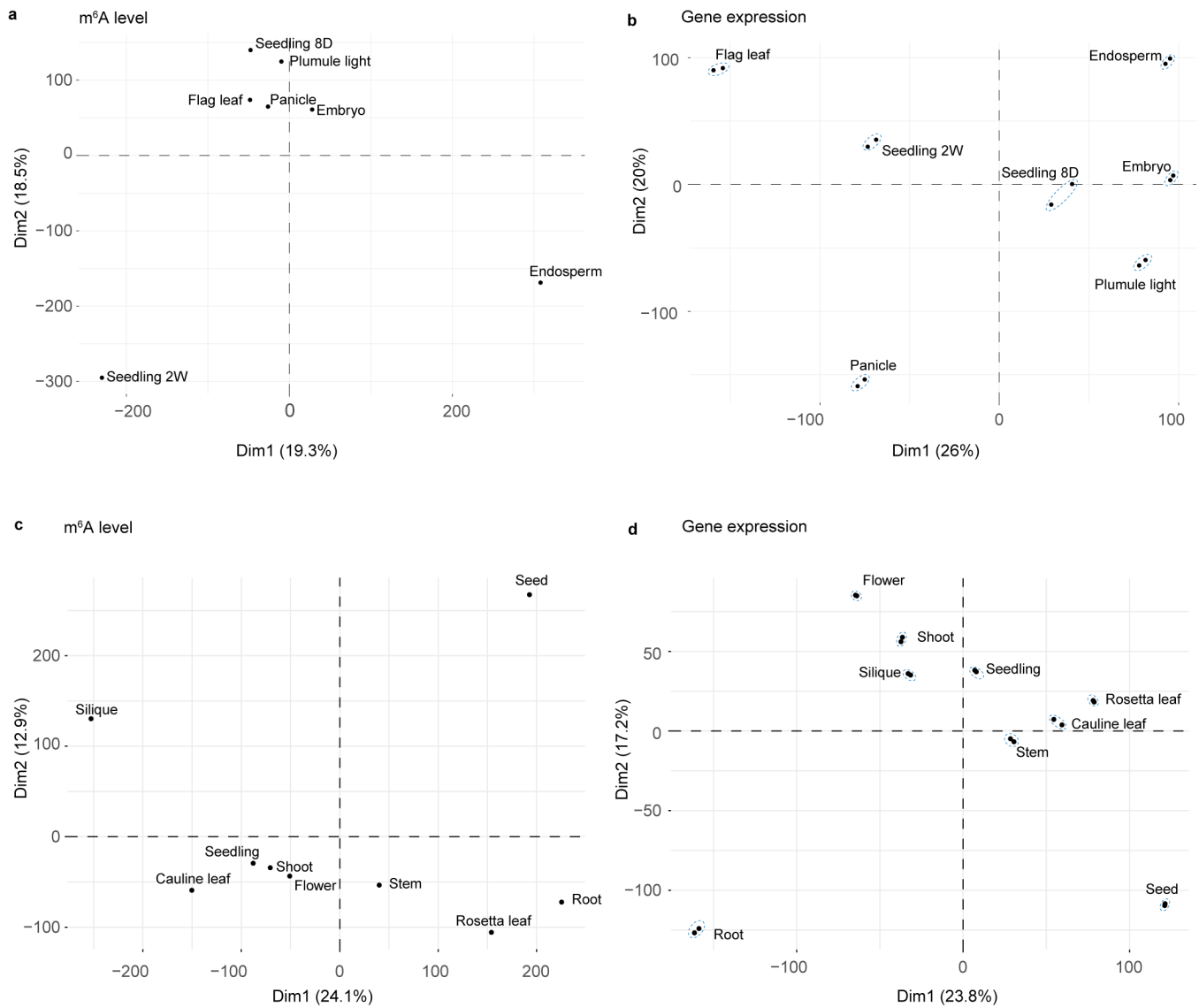


Supplementary Figures

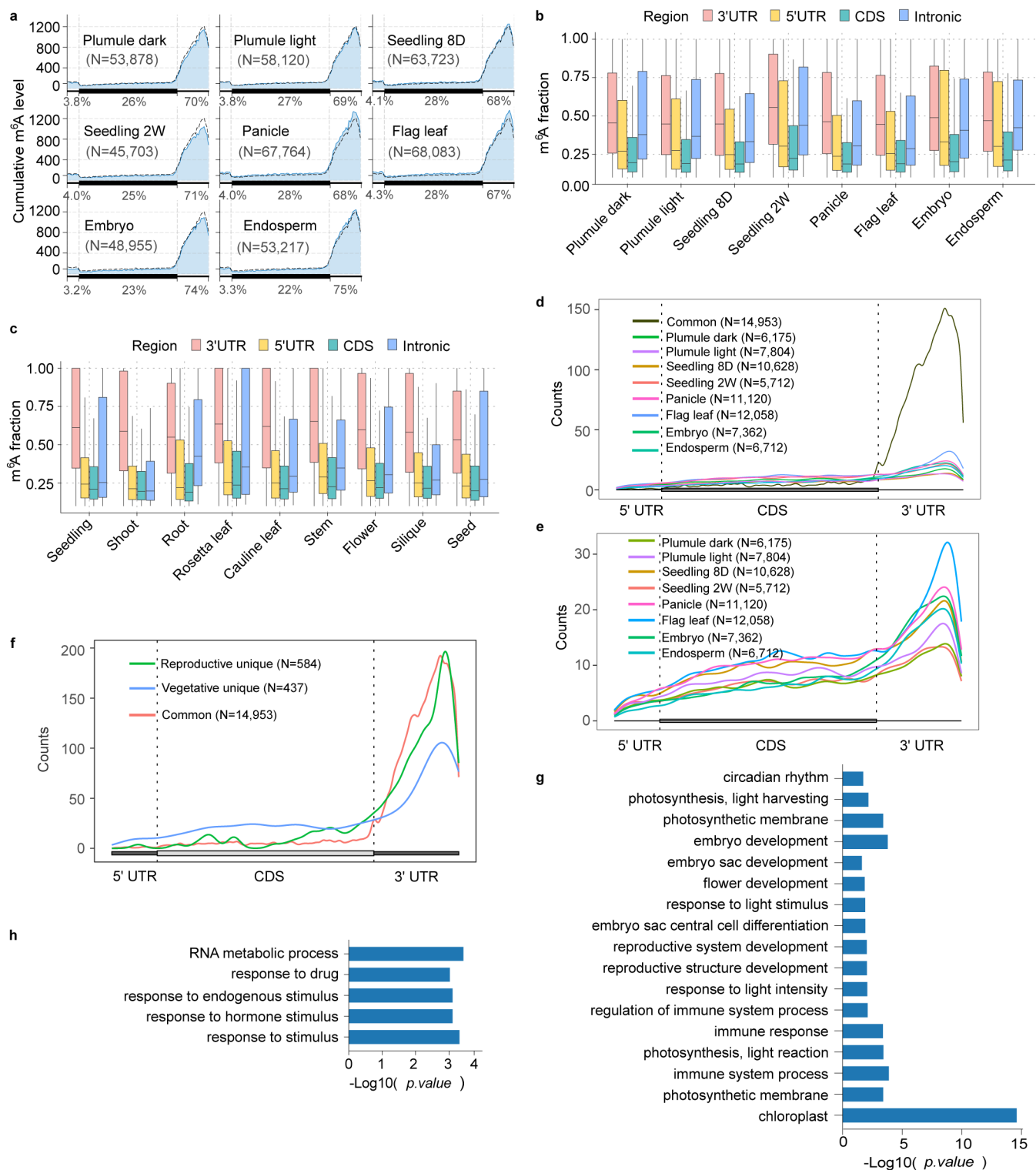


Supplementary Fig. 1: Overview of the quality of m⁶A-SAC-seq data.

a, The schematic diagram illustrating the m⁶A-SAC-seq protocol. **b**, Mutation ratios of A and m⁶A sites on spike-in probes with different motifs ($n = 256$), in treated (MjDim1 labeled) or untreated samples. The median value was marked as the black line in the box plot. GAC motif showed much higher mutation ratio than AAC motif. The P value was determined by one-tailed Wilcoxon rank-sum test. **c,d**, The relative conversion ratios in Arabidopsis tissues (**c**) and rice tissues (**d**). Two biological replicates were used. Data are means \pm SD, $n = 3$. **e**, Venn diagram showing the m⁶A sites detected by SAC-seq overlapped with those identified through miCLIP and DRS.



Supplementary Fig. 2: Principal component analysis (PCA) of m⁶A-SAC-seq data and RNA-seq data. **a,b, PCA of m⁶A fractions (**a**) and gene expression (**b**) in rice. **c, d**, PCA of m⁶A fractions (**c**) and gene expression (**d**) in *Arabidopsis*.**

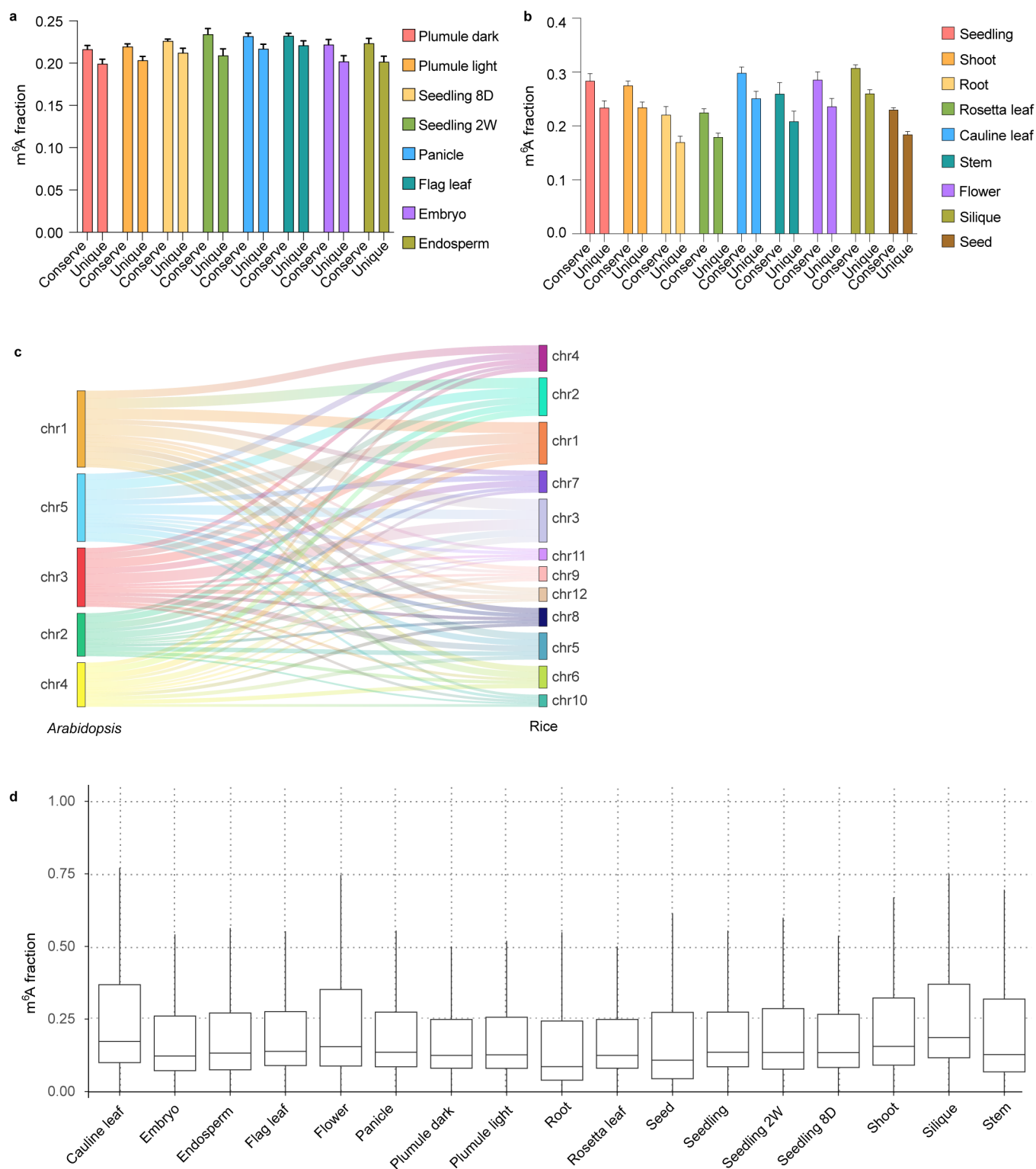


Supplementary Fig. 3: Tissue-specific m⁶A modification in various tissues of *Arabidopsis*.

a, Metagenes profile showing the m⁶A sites of nine *Arabidopsis* tissues distributed across transcript. The black dash line is the average m⁶A fraction among the nine tissues. The m⁶A site number (N) is indicated in the figure. The percentage of m⁶A fraction distributed in 5' UTR, CDS, and 3' UTR regions within different tissues is shown.

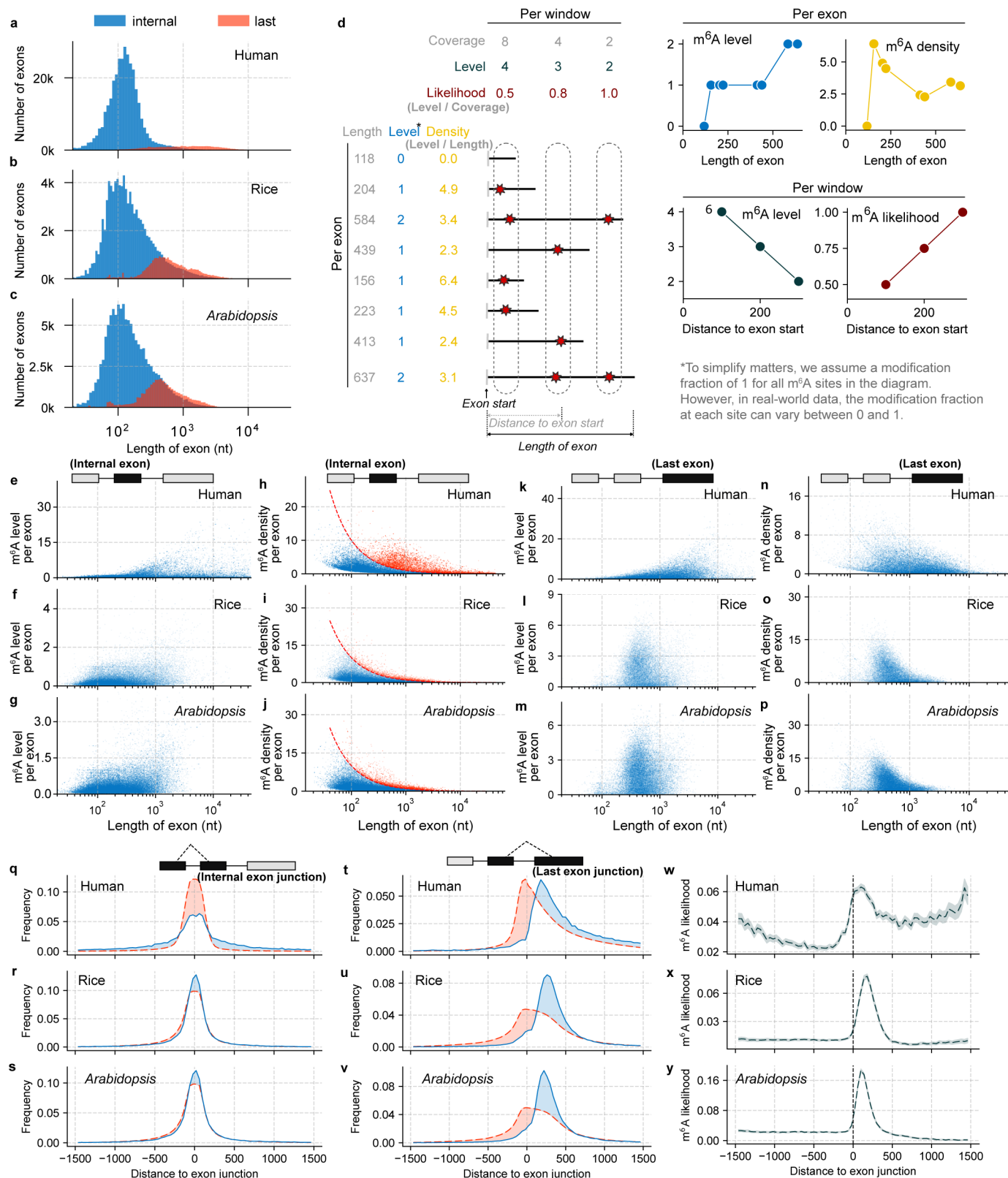
b, c, m⁶A fraction in different rice tissues (**b**) and *Arabidopsis* tissues (**c**) as showed in the 5' UTR, CDS, intronic and 3' UTR regions. **d, e**, Metagenes profile showing shared m⁶A sites and tissue unique m⁶A sites among rice tissues distributed across transcript (**d**), and the metagenes profiles of tissue unique m⁶A sites were also displayed separately in (**e**). The m⁶A site number (N) is indicated in the figure. **f**, Metagenes profile showing common-,

reproductive unique- and vegetative unique- m⁶A sites distributed across transcript. Tissues of panicle, embryo and endosperm were combined as the reproductive tissue, while the other tissues were combined as the vegetative tissues. Each transcript is divided into three parts: 5' UTR, CDS and 3' UTR. The m⁶A site number (N) is indicated in the figure. **g**, GO enrichment analysis of genes carrying reproductive unique m⁶A modification sites. **h**, GO enrichment analysis of genes containing vegetative unique m⁶A modifications. For **g** and **h**, One-sided Fisher's exact test. Adjusted *P* values using the linear step-up method.



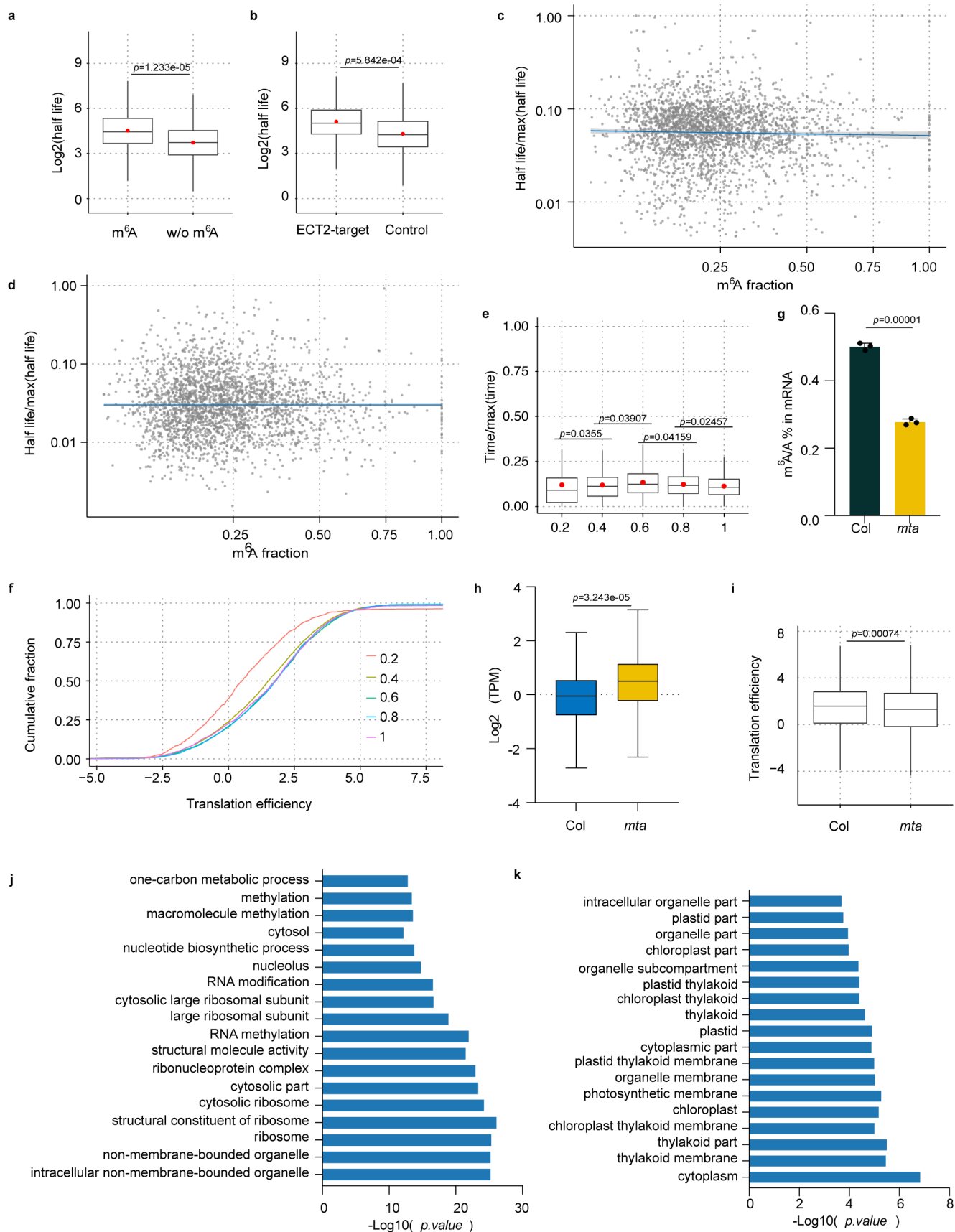
Supplementary Fig. 4: Conserved m⁶A site pairs across rice and *Arabidopsis* orthologue genes.

a, m⁶A fractions of rice unique sites compared to the rice-*Arabidopsis* conserved sites in rice. Data are means \pm SD, $n = 2$. **b**, m⁶A fractions of *Arabidopsis* unique sites compared to the rice-*Arabidopsis* conserved sites in *Arabidopsis*. Data are means \pm SD, $n = 2$. **c**, Sankey plot showing the correlation of these conserved m⁶A site pairs in orthologue genes of rice and *Arabidopsis*. **d**, m⁶A fractions of these conserved m⁶A site pairs in orthologue genes of rice and *Arabidopsis* within different tissues. In box plots, the center line represents the median. Upper and lower quartiles were the box limits.



Supplementary Fig. 5: Detailed analysis of m⁶A levels and exon lengths in plant and mammalian genomes.
a-c, Average exon lengths in the genomes of human (**a**), rice (**b**) and *Arabidopsis* (**c**) in regarding to last exons and internal exons. **d**, Diagram outlines the definition of 'm⁶A density' per exon and 'm⁶A likelihood' per sliding window. For 'm⁶A density,' the sum of all detected m⁶A sites within each exon is normalized by the exon length. The diagram illustrates that the level of m⁶A per exon may increase with the length of the exon, but the trend in 'm⁶A density' can decrease if the rate of m⁶A accumulation is slower than the rate at which exon length increases.

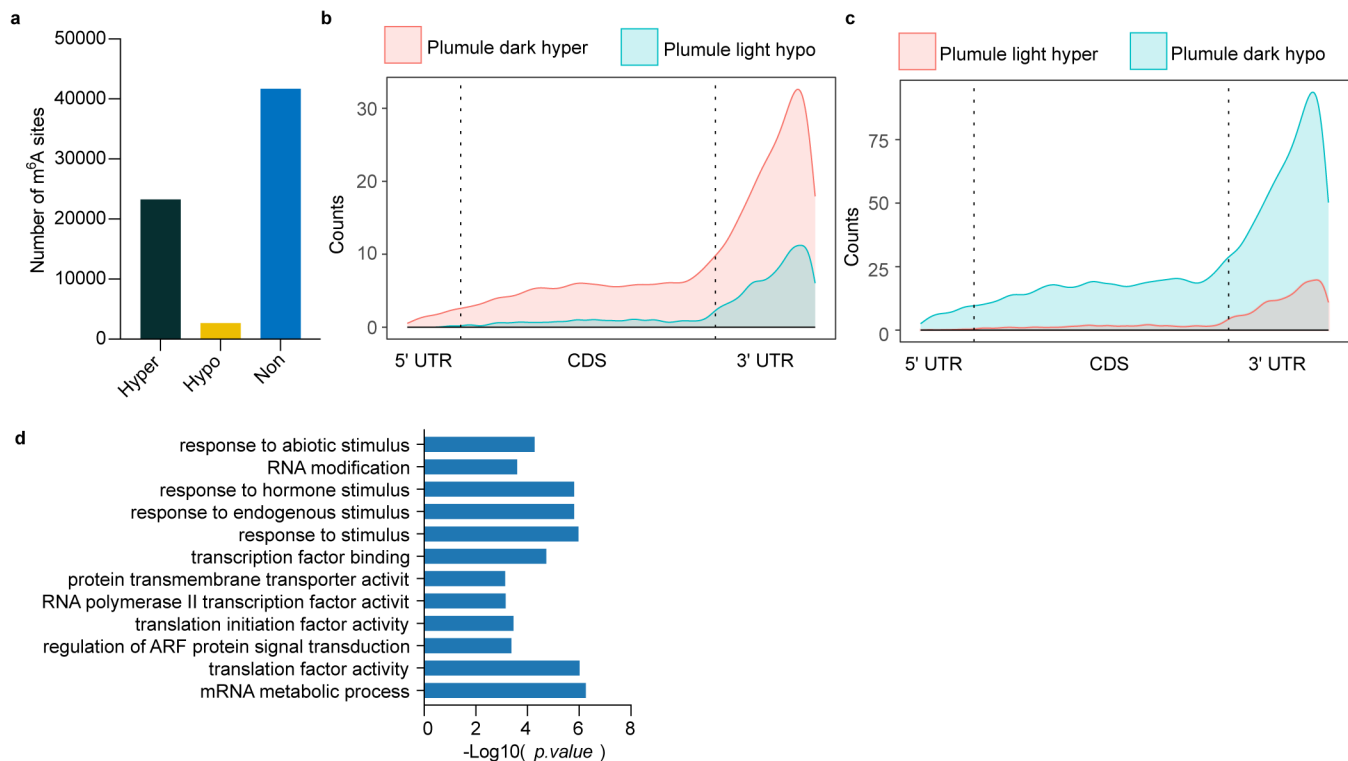
For 'm⁶A likelihood,' exons are aligned at their junction sites, and the overall 'm⁶A level' for each sliding window, starting from these junction sites, is calculated. The pileup coverage of these aligned exons is also calculated within each sliding window. 'm⁶A likelihood' is then defined as the ratio of the 'm⁶A level' to the exon coverage within the same window. The diagram indicates that 'm⁶A likelihood' may show an increasing trend even if the 'm⁶A level' is increasing at a slower rate than the decrease in exon coverage. **e-g**, m⁶A levels of each internal exon of the human (**e**), rice (**f**) and *Arabidopsis* (**g**) genomes were plotted against exon length. **h-j**, m⁶A density in the internal exons of human (**k**), rice (**l**), and *Arabidopsis* (**m**) transcripts were shown against exon length, represented by blue dots. m⁶A density was calculated as the total modification level of all m⁶A sites within each exon, normalized by exon length and multiplied by 1,000. Long exons with m⁶A density showing unusually elevated levels of m⁶A methylation (level per exon > 1) are highlighted in red. **k-m**, Analysis similar to panels **e-g**, but focusing on m⁶A levels and lengths for last exons. **n-p**, Similar to panel **h-j**, but the m⁶A density in last exons were shown. **q-s**, Frequency distribution of cumulative exon coverage relative to the internal exon junction sites was plotted in red line, and the frequency distribution of cumulative modification levels for all m⁶A sites were plotted in blue line. Regions where exon coverage exceeds m⁶A levels in frequency are shaded in red, and the opposite is shaded in blue. **t-v**, Analysis similar to panels **q-s**, but focusing on the last exons. **w-y**, Distribution of m⁶A site deposition likelihood near the stop codon in human (**w**), rice (**x**), and *Arabidopsis* (**y**) transcripts. Data are presented as median values.



Supplementary Fig. 6: Effects of m⁶A on the modified RNAs.

a, m⁶A modified transcripts showed higher lifetime than the unmodified transcripts. m⁶A, n = 7,77; w/o m⁶A, n = 3,319; **b**, higher lifetime of ECT2 targets with m⁶A modification than those not targeted by ECT2. ECT2-

target, n=584; Control, n=13,944. **c**, No significant correlation of non-3' UTR m⁶A modification levels with mRNA lifetime showed in scatter plot. **d**, Scatter plot showing correlation of non-3' UTR m⁶A modifications with mRNA lifetime using mRNA decay data set GSE118462. **e**, Box plots showing the lifetime distribution of 3' UTR m⁶A modification with mRNA lifetime using mRNA decay data set GSE118462. Transcripts were grouped into five categories (0,0.2); (0.2, 0.4); (0.4, 0.6); (0.6, 0.8); and (0.8, 1)) based on the sum of their m⁶A fractions. (0,0.2), n=76; (0.2, 0.4), n=265; (0.4, 0.6), n=463; (0.6, 0.8), n=588; (0.8, 1), n=710. **f**, Correlation of transcripts modified by non 3'UTR m⁶A sites with translation efficiency. Transcripts were grouped into five categories (0,0.2); (0.2, 0.4); (0.4, 0.6); (0.6, 0.8); and (0.8, 1)) based on the sum of their m⁶A fractions. (0,0.2), n=1,003; (0.2, 0.4), n=4,319; (0.4, 0.6), n=4,819; (0.6, 0.8), n=2,415; (0.8, 1), n=1,418. The *Arabidopsis* seedling translation efficiency data set [GSE206292](#) was used for the analysis. **g**, *Arabidopsis mta* mutant showed significant reduced mRNA m⁶A levels. The m⁶A-to-A ratio was determined using calibration standards. Data are means \pm SD, $n=3$. Student t-test was used to determine the statistic difference. **h**, Transcript levels of genes associated with reduced m⁶A modifications in *mta* mutant compared with the wild type (Col). **i**, Translation efficiency of *mta* mutant was reduced on average. Translation efficiency data set [GSE206292](#) was used for the analysis. **j**, GO enrichment analysis of genes with upregulated translation efficiency mediated by MTA. **k**, GO enrichment analysis of genes with downregulated translation efficiency mediated by MTA. For **j** and **k**, One-sided Fisher's exact test. Adjusted *P* values using the linear step-up method. For **a**, **b**, and **e-i**, the *P* value was determined by one-tailed Wilcoxon rank-sum test. For box plots of **a**, **b**, **e**, **h**, and **i**, the center line represents the median, and the red dot represents the mean. Upper and lower quartiles were the box limits.



Supplementary Fig. 7: Light responsive m⁶A modification in rice and MTA regulated m⁶A sites in *Arabidopsis*.

a, Number of hypermethylated (hyper) and hypomethylated (hypo) m⁶A sites in rice induced by light. **b,c**, Metagene profile showing hypermethylated- (**b**) and hypomethylated (**c**) m⁶A sites induced by light distributed across transcript. Each transcript is divided into three parts: 5' UTR, CDS and 3' UTR. **d**, GO enrichment analysis of genes containing hypermethylated m⁶A sites induced by light. One-sided Fisher's exact test. Adjusted *P* values using the linear step-up method.